First publ. in: Science 309 (2005), 5743, pp. 2043-2045

Jumping Nanodroplets

A. Habenicht,[1] M. Olapinski,[2] F. Burmeister,[3]
P. Leiderer,[1] J. Boneberg[1]

Flat gold nanostructures on inert substrates like glass or graphite were illuminated by single intensive laser pulses with fluences above the gold melting threshold. The liquid structures produced in this way are far from their equilibrium shape, and a dewetting process sets in. On a time scale of a few nanoseconds, the liquid contracted toward a sphere. During this contraction, the center of mass moved upward, which could lead to detachment of droplets from the surface due to inertia. The resulting velocities were on the order of 10 meters per second for droplets with radii in the range of 100 nanometers.

When small droplets impinge on a surface, varying degrees of deposition can be observed, ranging from sticking to rebounding. Sticking is essential for ink-jet printing and in agricultural agents that function by sticking to leaves; rebounding is desirable in cases such as self-cleaning surfaces (*1*, *2*).

The physics of impacting droplets has been well studied (*3*–*5*), and various types of (macroscopic) droplet sources have been developed (*6*). The impact-rebound process can be described energetically as the transformation of the impinging drop's kinetic energy (KE) into surface deformation energy, followed by the inverse process, which detaches the drop (*7*).

We examined whether it is possible to begin with deformed droplets on a surface and observe only the transformation from surface deformation energy to KE, as indicated by droplets jumping off the surface. For this purpose, we used droplets in the submicrometer range, which are much smaller than those typically used in impact studies. Such droplets can readily be obtained in an energetically unfavorable pancakelike shape with a large surface-to-volume ratio by preparing nanostructures in the solid state (e.g., by evaporation) on a substrate that in equilibrium is not wetted by the deposited material. Upon melting the nanostructures with a short laser pulse, dewetting sets in, and under appropriate conditions, detachment of the resulting droplets can be observed.

The gold nanostructures we used here were fabricated by colloidal lithography, in which a monolayer of monodisperse spherical particles (with diameters of 1.5 to 3 μm) serves as a deposition mask (*8*, *9*) to produce flat gold triangles with side lengths between 400 and 800 nm (Fig. 1A). The thickness of the evaporated films ranged between 50 and 160 nm. After removal of the colloid mask, these triangular gold structures were irradiated with a frequency-doubled Neodymium Doped Yttrium Aluminum Garnet (Nd:YAG)–laser (wavelength λ = 532 nm, full-width at half maximum of 10 ns). Because the absorption length of the laser radiation is smaller than the thickness of the nanostructure, we have to consider the temperature distribution inside of the nanostructure. An estimate for the thermal diffusion lengths on the time scale of the laser pulse yields 1600 nm for solid gold and 900 nm for molten gold, which is well above the thickness of the structures used here (*10*). Thus, we can assume that the temperature stays almost homogeneous over the whole volume of each nanostructure.

First, the dewetting of the initially solid triangular gold structures (thickness 50 nm, side length 800 nm; Fig. 1A) on highly orientated pyrolytic graphite (atomically smooth with rare steps) upon melting was studied in ambient conditions. This system exhibits nearly complete nonwetting in equilibrium; the contact angle is 131° (*11*).

After heating with a laser pulse, the metal triangles in Fig. 1A become molten for a certain amount of time (in the nanosecond range) and then solidify again as a result of the heat loss into the substrate. The resulting solids provide insight into the nanostructures at the moment of solidification (Fig. 1B). The laser fluence (energy density) was not constant but increased from the top left toward the bottom right of Fig. 1B. The duration of the molten state is longer along the indicated path, thus providing a sequence of images of the development of the dewetting process from flat triangles toward spherical structures (Fig. 1C).

The dewetting process starts at the corners of the triangles, where the radius of curvature is small and the force due to surface tension is high. The bumps that form there move toward the center, where they converge. In this manner, surface energy is transformed into KE, and the initially horizontal flow is directed upward.

The dewetting dynamics of the nanostructures are comparable to the growth of holes in thin liquid metal films (*12*, *13*), where the low viscosity of these systems allows inertia to play a dominant role, as described by the formula for the retraction velocity given by Brochard-Wyart (*14*), $v = (2|S|\rho_l^{-1}d^{-1})^{0.5}$, in which S is the spreading coefficient (1.904 N/m), ρ_l is the density of liquid gold, and d is the thickness of the metal layer. With these values, we obtained retraction velocities in the range of 65 m/s, implying a time scale on the order of 10 ns for the transition toward a sphere; preliminary time-resolved reflectivity experiments that we used to monitor this transition confirm this estimate.

In the dynamics of our liquid nanostructures, inertia dominates over viscous dissipation. Given this, can the droplets detach from the surface, as they do in the second half of the impact-rebound process observed in macroscopic drops? Such a detachment could happen if the KE of the droplet's center of gravity perpendicular to the surface surmounts the adhesion energy, taking into account dissipative losses. The upper right part of Fig. 2 shows that all of the particles are indeed missing. Apparently, detachment readily takes place if the laser fluence is slightly above the value

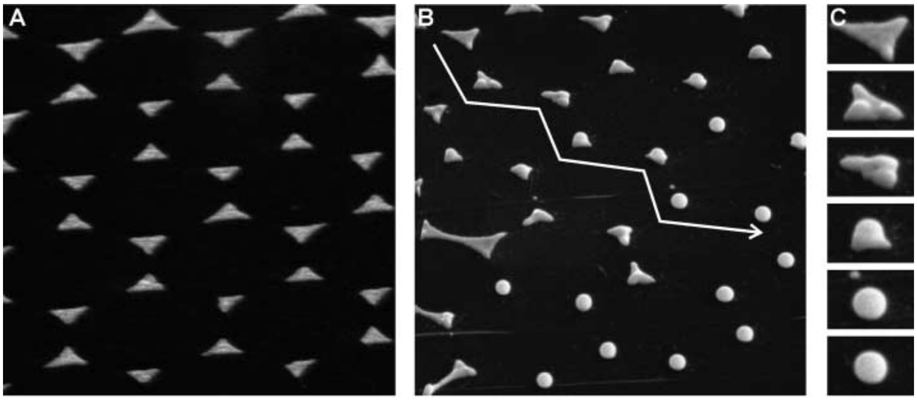

Fig. 1. (**A**) Scanning electron microscope picture of triangular gold nanostructures on highly orientated pyrolytic graphite, as produced by colloidal monolayer lithography, before laser annealing (substrate tilted, image size 8 × 16 μm). (**B**) The same nanostructures after annealing with a nanosecond laser pulse and resolidification. Along the arrow the laser fluence and thus the duration of the molten state increased. The resulting solid nanostructures therefore represent different stages of the dewetting process (**C**).

[1]Department of Physics, University of Konstanz, Universitätsstrasse 10, 78457 Konstanz, Germany. [2]Department of Physics and Center for Nanoscience, Ludwig-Maximilians-Universität München, Geschwister-Scholl-Platz 1, 80539 München, Germany. [3]Fraunhofer Institute for Mechanics of Materials, Woehlerstrasse 11-13, 79108 Freiburg, Germany.

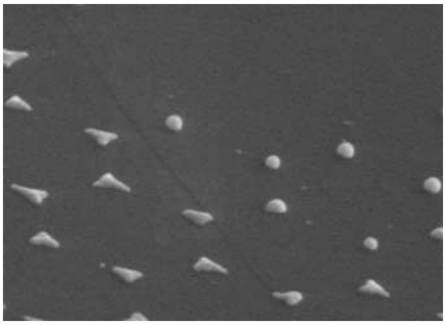

Fig. 2. Laser-molten gold nanostructures on graphite, similar to Fig. 1. In this case, the laser fluence increased from bottom left to top right of the picture. The region where spherical particles formed is quite narrow, and at higher laser fluence the particles have left the surface. Substrate tilted, image size 8 × 12 μm.

necessary for the triangles to stay melted long enough to contract to spheres.

To study the detachment in more detail, we placed our samples in a vacuum chamber and used glass as the substrate (with a root-mean-square roughness of 3 nm) instead of graphite for the gold triangles [contact angle of 140° for SiO_2 (*15*)]. The structures were irradiated with the laser beam from the substrate side. In spite of these changes, the effects described above remained the same. For the determination of the detachment velocity, we used a thin plane of light (provided by an argon laser, wavelength λ = 488 nm, power P = 500 mW) parallel to the substrate at a distance of several millimeters. As particles crossed the light sheet, we monitored scattering with a photomultiplier. From the known distance of the light sheet to the surface, the scattering data can be converted into a velocity distribution.

In Fig. 3A, triangles with a side length of 405 nm and a height of 95 nm were used, which created spheres with a radius R of 120 nm. The particles left the surface with an average velocity (±SD) of 19 ± 2 m/s. When the incident laser fluence was varied (Fig. 3B), a sharp critical value F_C was found, below which the particles did not detach. For fluences greater than F_C, the velocity of the particles remained essentially constant at v = 20 m/s up to about $2F_C$, and then gradually started to increase.

This behavior is in support of the dewetting-induced detachment mechanism outlined above: The velocity is gained from conversion of surface energy to KE, which should be independent of laser fluence. Only at the highest energy densities did the particles pick up considerably more speed, an effect which we attribute to partial evaporation of the particles and thus an additional acceleration created by recoil in front of the substrate. In this higher fluence range, the estimated temperature of the particles reached values above the boiling point of gold (3129 K).

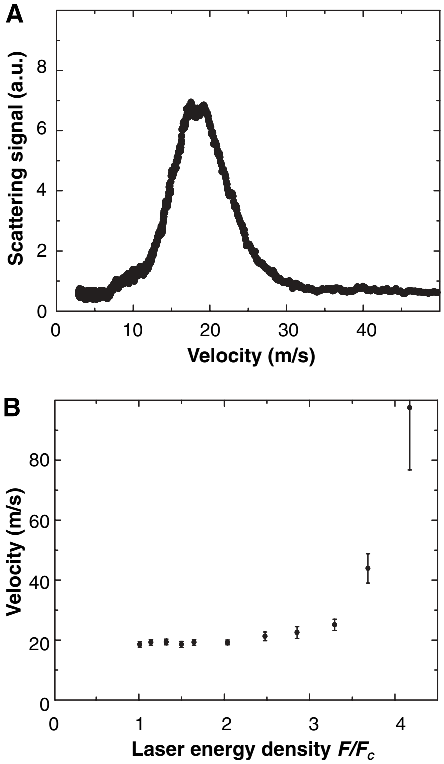

Fig. 3. (**A**) Velocity distribution of particles jumping off the surface, resulting from laser melting of gold triangles with a side length of 405 and 95 nm in height. Here, the laser fluence was a factor of 2 above the threshold value F_C, and the signal was averaged over four time-of-flight measurements on virgin substrate areas. a.u., arbitrary units. (**B**) Velocity of the detached particles versus the reduced laser fluence F/F_C. Error bars show means ± SD.

Also in agreement with the interpretation of dewetting-induced detachment is the dependence of the velocity on the initial structure height (at a fixed lateral size of 405 nm, Fig. 4): Structures with a larger height have a smaller surface-to-volume ratio and thus reach lower velocities.

For an estimate of the conversion from potential to KE, we consider first the change in surface energy ΔE_S of the flat structure in the initial state toward the detached droplet. It is given by

$$\Delta E_S = \gamma_{lv}\left((1-\cos\theta)\frac{\sqrt{3}}{4}k^2 + 3kd - 4\pi R^2\right)$$

where γ_{lv} is the liquid-vapor surface tension of gold [1.15 N/m (*16*)]; θ is the contact angle of liquid gold on glass; k and d are the side length and the thickness, respectively, of the initial triangular structure; and R is the radius of the detached droplet. Here, we have made use of Young's equation, $\gamma_{sl} - \gamma_{sv} = -\gamma_{lv}\cos\theta$, where γ_{sl} is the surface energy density of the solid-liquid interface (*17*). Assuming that evaporation can be neglected (i.e., $\frac{\sqrt{3}}{4}k^2 d = \frac{4}{3}\pi R^3$), the KE of a droplet with velocity v, $E_{kin} = \frac{\sqrt{3}}{8}k^2 d\rho v^2$, where ρ is the density of

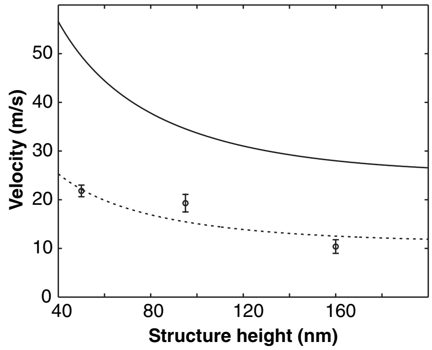

Fig. 4. Droplet velocity obtained upon laser melting of triangular nanostructures with a side length of 405 nm and various heights. The data points show the measured velocity in the low laser fluence regime ($F_C < F < 2.5F_C$). The solid line represents a calculation for 100% conversion of excess surface energy to KE; the dotted line is a fit to the experimental data with an energy conversion of 20%. Error bars show means ± SD.

gold, can be directly compared with ΔE_S. The result as a function of structure height is plotted in Fig. 4, showing that for these particles the conversion ratio from surface energy to translational KE is on the order of 20%. Other channels for energy conversion not considered here are the excitation of droplet oscillations and dissipative friction effects.

Because the shape of the nanostructures at the beginning of the dewetting process can be chosen at will (e.g., by preparing the structures by electron beam lithography), one can tailor the flow in these structures for many different geometries. Furthermore, laser annealing allows the freezing of the liquid in different stages of the development and thus the application of scanning microscopy techniques. Therefore, this approach opens a wealth of possibilities for studying the dynamics of liquids on the nanoscale, including droplet impact on surfaces.

References and Notes

1. J. Klein, *Nature* **405**, 745 (2000).
2. H. Sirringhaus *et al.*, *Science* **290**, 2123 (2000).
3. A. M. Worthington, *Proc. R. Soc. London* **25**, 261 (1876).
4. I. V. Roisman, R. Rioboo, C. Tropea, *Proc. R. Soc. Lond. Ser. A* **458**, 1411 (2002).
5. R. Rioboo, M. Marengo, C. Tropea, *Exp. Fluids* **33**, 112 (2001).
6. M. Rein, *Fluid Dyn. Res.* **12**, 61 (1993).
7. R. Richard, D. Quéré, *Europhys. Lett.* **50**, 769 (2000).
8. F. Burmeister *et al.*, *Langmuir* **13**, 2983 (1997).
9. F. Burmeister *et al.*, *Appl. Surf. Sci.* **144-145**, 461 (1999).
10. We calculated the thermal diffusion length as $(2\kappa\tau C^{-1}\rho^{-1})^{1/2}$, where κ is the thermal conductivity (317 W m^{-1} K^{-1} solid and 106 W m^{-1} K^{-1} liquid), τ is the duration of the laser pulse, C is the specific heat (129 J kg^{-1} K^{-1} solid and 149 J kg^{-1} K^{-1} liquid), and ρ is the density of gold (19.3 g cm^{-3} solid and 17.2 g cm^{-3} liquid).
11. U. Gangopadyay, P. Wynblatt, *Mat. Res. Soc. Symp. Proc.* **318**, 393 (1994).
12. J. Bischof, D. Scherer, S. Herminghaus, P. Leiderer, *Phys. Rev. Lett.* **77**, 1536 (1996).
13. S. Herminghaus *et al.*, *Science* **282**, 916 (1998).
14. F. Brochard-Wyart, *J. Phys. II France* **3**, 21 (1993).

15. J. V. Naidich, in *Progress in Surface and Membrane Science*, D. A. Cadenhead, C. F. Danielli, Eds. (Academic Press, New York, 1981), vol. 14, pp. 353–484.
16. I. Egry, G. Lohoefer, G. Jacobs, *Phys. Rev. Lett.* **75**, 4043 (1995).
17. C. Ukiwe, D. Y. Kwok, *Langmuir* **21**, 666 (2005).
18. We are grateful for the experimental contributions by S. Rottmair at the early stages of this work. We acknowledge financial support by the Deutsche Forschungsgemeinschaft within the SFB 513, Project B1 and the Landesstiftung Baden-Württemberg within the Network of Competence "Functional Nanostructures," Project B2.

23 June 2005; accepted 22 August 2005
10.1126/science.1116505